Effects of water sorption on Poly(lactic acid)

Roberto Pantani[*,a], Felice De Santis[a], Finizia Auriemma[b], Claudio De Rosa[b], Rocco Di Girolamo[b]

[a]*Dipartimento di Ingegneria Industriale, Università di Salerno, 84084 Fisciano (SA), Italy;*

[b]*Dipartimento di Scienze Chimiche, Università di Napoli "Federico II", 80126 Napoli, Italy*

Roberto Pantani

University of Salerno,

Department of Industrial Engineering,

Via Giovanni Paolo II, 132 - 84084 - Fisciano (SA)

E-mail: rpantani@unisa.it

Phone: +39 089 96 4141

Abstract

When in contact with water, poly(lactic acid), PLA, undergoes severe physical changes. Hydrolysis is obviously the most expected and studied one, and it is followed by weight loss. However, other phenomena occur such as opacification and crystallization. Although these phenomena are sometimes reported in the literature, apart from hydrolysis which has been thoroughly studied at several temperatures, the other ones have not been deeply analyzed and their timescales have not been so far determined. This work aims at studying the physical changes induced by water sorption to PLA, by analyzing the physical changes taking place in solid samples immersed in water for different times (starting from a few hours) and at temperatures close to the glass transition. The obtained results allow determining the timescales of the different phenomena and thus the possible cause-effect relationship among them. In particular, it is shown that opacity is the first phenomenon to become evident, on a timescale consistent with water sorption, and seems to be due to crazes induced by water. The second phenomenon to become evident is the crystallinity evolution, which is shown to be consistent with a heterogeneous nucleation on the crazes. These two phenomena take place before hydrolysis becomes significant, thus raising doubts about the fact that hydrolysis can be their cause.

Keywords

Opacification –water sorption – poly(lactic acid)

Introduction

Poly(lactic acid) (PLA) is a biodegradable polymer offering several smart features that make it highly competitive with conventional non-biodegradable materials, such as the processability by standard techniques and good mechanical properties [1]. The biodegradability, even being one of the most important features of this material, makes it quite sensitive during stocking and for narrow processing conditions [2-4]. Furthermore, in the presence of water, poly(lactic acid) experiences important physical modifications: water plasticizes and swells the material, its glass transition temperature is lowered and mobility and thus crystallization kinetics is augmented. On a longer timescale, the hydrolysis reduces the molecular weight [5]. The hydrolytic degradation, above all, has been deeply studied [6-10] and the main factors affecting this phenomenon are quite well defined. On checking the literature, surprisingly, it can be noticed that when temperatures close to the glass transition of PLA are studied, the effects of water are mostly assessed at times when the hydrolysis already induced significant changes in the material, namely after a few days [7, 11]. Obviously, this makes it difficult to understand to which extent other phenomena which take place inside the material (opacification [12], crystallinity evolution [7]) are due to hydrolysis, or vice versa can develop independently. This work aims at studying the physical changes induced by water sorption to PLA at short times (of the order of a few hours) and at relatively high temperatures (close to the glass transition), in order to analyze the timescales of some of the phenomena taking place in PLA in the presence of water.

Experimental

In this work, the poly(lactic acid) is the resin Ingeo 4032D provided by NatureWorks LLC. This grade is designed for film casting, having D-isomer content= 1.4% and it was previously characterized [5]. The glass transition temperature (T_g) and the melting point temperature (T_m) of PLA 4032D are about 60 °C and 155 °C, respectively. The film samples, with a thickness of about 400 μm, were obtained by compression molding by means of a Carver laboratory press (190 °C, 5 min, then quenched). The film samples resulted being completely amorphous and they were used for the subsequent experimental tests. The temperature range analyzed in this work is very close to the glass transition temperature in order to accelerate the phenomena. Furthermore, it has to be mentioned that the temperature of 58 °C is the one considered as a standard for the biodegradation tests of PLA [13].

The analysis of water sorption and diffusion was carried out using a DVS Advantage-2 microbalance (Surface Measurement Systems Ltd.). This device allows following the sample weight while the temperature and the water partial pressure in the nitrogen atmosphere surrounding the sample are kept constant. In this work the sample was submitted to steps of water partial pressure increase, at a constant temperature. The steps were long enough to allow equilibrium at each of the chosen partial pressures. The obtained data were analyzed according to the methods described in the literature [14] and allowed to determine the equilibrium water content at each relative humidity (RH) and the diffusivity of water inside the samples as a function of the equilibrium water content.

Dynamic mechanical properties were evaluated using a PerkinElmer DMA8000. Measurements were conducted at a constant frequency (1 Hz) and amplitude (5 μm) in tensile mode on films 400 μm thick. Some tests were conducted by keeping the sample in water both at constant temperature (58 °C) and during heating at a rate of 2 °C/min. Other tests were conducted in the conventional air oven, during heating at the same rate (2 °C/min).

The samples were kept immersed in bidistilled water at constant temperature. Three temperatures were adopted: 50 °C, 54 °C and 58 °C. Other samples were kept at 58 °C in solutions of water and Calcium Nitrate tetrahydrate, supplied by Sigma Aldrich. Calcium Nitrate has a very high solubility in water, larger than 1 kg/l, and allows to obtain solutions with densities larger than 1.2. Two salt solutions were obtained, having densities of 1.05 g/cm³ and of 1.1 g/cm³. The presence of the salt reduces the activity of liquid water, thus allowing to monitor the phenomenon due to water sorption in the same conditions but at a lower equilibrium water content. The equilibrium water content of the samples was assessed by leaving a 400 μm thick film of known dry weight in solution at 58 °C for about 5 h. The sample was then taken out from the solution, cleaned with a dry cloth and weighed [15]. The water content could thus be assessed and the results are reported in Table 1. The water absorbed by the polymer decreases on increasing the salt concentration (namely on increasing the solution density).

Table 1. Equilibrium water content and concentration, C_{A0}, for samples immersed in solutions of water and Calcium Nitrate tetrahydrate at 58 °C

Density of the solution (at 23 °C) in g/cm³	Equilibrium water content at 58 °C in g/(100g of dry polymer)	C_{A0} (mol/m³)

1 (pure water)	1.49	993
1.05	1.44	960
1.1	1.29	860

At selected time intervals, some samples were taken out from the liquid, washed with pure water and dried at room temperature for about 5 h before any further analysis was carried out. The opacity of the films was measured by using a Konica Minolta X-Rite SP60 Series Spectrophotometer. Following the ASTM Book of Standards E 284 "Terminology of Appearance", opacity is the ability of a thin film or sheet of material to hide a surface behind and in contact with it, expressed as the ratio of the reflectance factor R_b when the material is backed by a black surface to the reflectance factor R_w when it is backed by a white surface (usually having a reflectance factor of 0.89).

$$O_p = \frac{R_b}{R_w} \times 100 \tag{1}$$

The Differential scanning calorimetry (DSC) analysis was performed on samples with a mass ranging between 5 and 7 mg. The tests were carried out by means of a Mettler Toledo DSC 822 under a nitrogen atmosphere. The samples were heated from 25 °C to 200 °C at 10 °C/min.

Density measurements were carried out by means of a density gradient column containing solutions of water and calcium nitrate tetrahydrate. The columns were kept at 25 °C and calibrated with four floats of known density.

Intrinsic viscosity, [η], was measured in chloroform at a polymer concentration of C=0.1 g/dl and at 30 °C using a Cannon-Ubbelohde viscometer. The intrinsic viscosity of each sample was calculated by using the Solomon-Ciuta equation [16, 17] of a single point measurement:

$$[\eta] = \sqrt{2}\left[t/t_0 - 1 - \ln\left(t/t_0\right)\right]^{1/2} / C \tag{2}$$

where t is flow time of solution, t_0 is flow time of pure solvent.

The Mark-Houwink equation was then used to determine the molecular weight:

$$M_v = \left([\eta]/k\right)^{1/a} \tag{3}$$

The constants for PLA are k=2.21×10^{-4} dl/g and a=0.77 [18]. A minimum of 5 samples taken from the same specimen were analyzed.

Wide and Small angle X-ray scattering (WAXS/SAXS) data of the PLA samples were collected at room temperature using a Kratky compact camera SAXSess (Anton Paar, Graz, Austria) in the slit collimation configuration, attached to a conventional X-ray source (CuKα, wavelength λ =1.5418 Å). The configuration allows collecting simultaneously the scattered radiation at the small and wide angle on a BAS-MS imaging plate (IP-FUJIFILM). The IP plates were processed with a digital imaging reader (Cyclone by Perkin Elmer). The range of sampled scattering vector modulus was 0.1 nm^{-1} $\leq q \leq 28$ nm^{-1}, where $q = (4\pi \sin\theta/\lambda)$ and 2θ is the scattering angle. After subtraction for the dark current, the empty sample holder, and a constant background due to thermal density fluctuations, the slit smeared data at low angle (in the q range 0.1-2 nm^{-1}) were de-convoluted with the primary-beam intensity distribution using the SAXSquant 2.0 software to obtain the corresponding pinhole scattering (desmeared) intensity distribution, using an iterative process, in the infinite slit approximation. WAXS data were not desmeared because at wide angle the infinite slit approximation was not applicable. However, for selected samples, we checked that the so obtained WAXS profiles contained the relevant information for the purpose of the present investigation which was equivalent to those obtained collecting diffraction data in a point collimation geometry.

The constant value of intensity approximating the background I_{back} was found by fitting the smeared SAXS intensity curve in the range $2 < q < 4$ nm^{-1} ($I(q_{\text{high}})$) with the function [19]:

$$I(q_{\text{high}}) = I_{\text{back}} + bq^{-3} \tag{4}$$

where I_{back} and b are fitting parameters.

Field emission scanning electron microscopy (FESEM) images were obtained with a FEI Nova NanoSEM 450 emission SEM equipped with an Everhart-Thornley detector (ETD) and a Through Lens Detector (TLD). Images were collected at an accelerating voltage of 1-5 kV (range of acceleration voltage: 50 V–30 kW).

The PLA films were analyzed both without and with imposing a basic hydrolysis treatment using water solutions containing 40 vol % methanol 0.5 M NaOH(aq) for 30 min at 58 °C and/or 10 min at 65 °C. After the reaction, the samples were washed with cold methanol and dried in a vacuum oven for 12 h at room temperature. The basic solution preferentially induces hydrolysis of the ester bonds located in the amorphous regions and enhances the visibility of the lamellar crystals in the FESEM micrographs. It was verified that the etching procedure does not induce changes in the crystallinity of the samples (see Appendix A. Supplementary data). All imaged samples were mounted on Al specimen mounts and coated

with a thin layer of Au-Pd in order to eliminate any undesirable charge effects during the FESEM observations.

Results and Discussion

Water sorption and diffusion

Fig. 1A reports the sorption curve of the films of PLA at the temperature of 58 °C. It is evident that at high humidity values (namely at high water partial pressures) the sorption curve deviates from linearity, following a Flory-Huggins mode of sorption. These isotherms are normally observed when the penetrant effectively plasticizes the polymer, being a strong solvent or swelling agent for the polymer, like is water for PLA matrix. No relevant hysteresis was observed during desorption (not reported in Fig. 1A).

The diffusivity was calculated during each sorption and desorption step, and is reported in Fig. 1B versus the equilibrium water content reached at the end of the step. The diffusivity is essentially independent of the water content, in agreement with previously reported results [20].

A   B
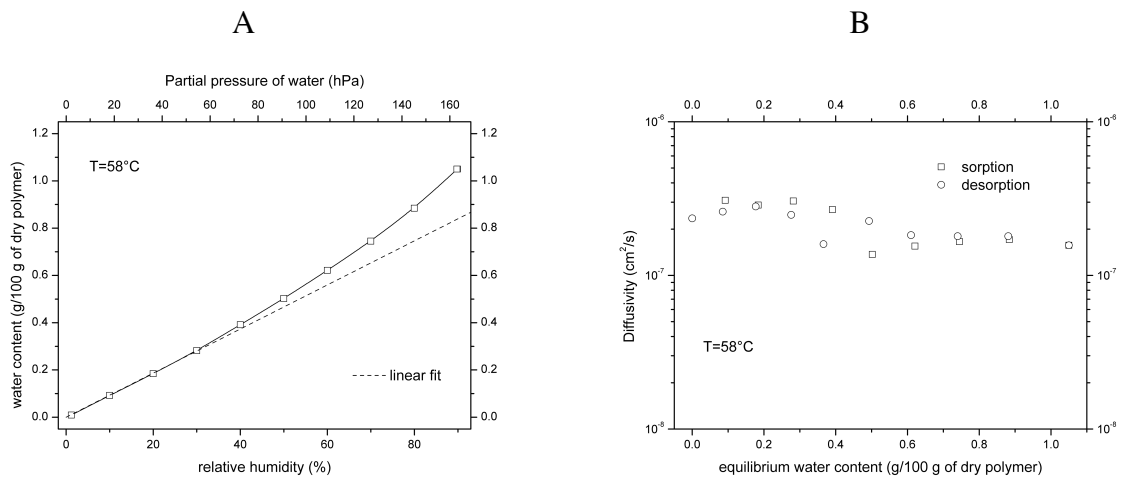
Fig. 1 Results of sorption-desorption tests: (A) Equilibrium concentration, C_{A0}, of water vapor (wt%) as function of partial pressure of water (Pa) during sorption steps; the dotted line refer to the linear fit of the points at the lowest RH; (B) Diffusion coefficient of water vapor (cm^2/s) as a function of water content.

Water diffusivity was found to be of the order 10^{-7} cm^2/s [21], which allows water to reach equilibrium inside samples 400 μm thick in a time of about 2 h. According to literature indications [14] the diffusivity of water in PLA decreases of about 25% for a temperature

decrease of about 10 °C. This would mean that in the range of temperatures analyzed in this work (from 50 °C to 58 °C) water reaches a homogeneous concentration in about 2 h in the 400 μm thick films. The test reported in Fig. 1 lasts about 3 days (~72 h). In this period, no significant changes were noticed in the sample. Even keeping the sample at the highest reached humidity (about 90%) for 100 h does not result in any evident change in the sample appearance.

Hydrolysis

When in contact with water, PLA can undergo hydrolytic scission of the chains. The rate of hydrolysis depends on many factors, including temperature. In a previous work [5] the hydrolytic degradation of the same PLA grade adopted in this work was followed during the time for films immersed in water at 58 °C. In particular, the molecular weight was measured at selected time intervals by adopting GPC measurements. The first measurement was taken after about 10 days of immersion, which means a time much longer with respect to the scale of evolution of the phenomena analyzed in this work. In order to assess the significance of hydrolytic scission at shorter times, the molecular weight of the samples was measured by intrinsic viscosity. The results are reported in Fig. 2 together with the mentioned literature data [5]. It can be noticed that the molecular weight measured by intrinsic viscosity, M_v, needed to be scaled by a factor of about 1.5 in order to have a superposition of the two sets of data (in particular the left and right axes in Fig. 2 are scaled according to this factor).

The data of molecular weight collected in this work were described assuming a kinetics of hydrolysis as follows [22]:

$$\frac{d}{dt}C_E = -K_h C_E C_A C_C \tag{5}$$

where C_E is the concentration of ester bonds, C_C the concentration of terminal carboxylic ends and C_A is the concentration of water (which is here assumed to be constant and equal to the equilibrium value reported in Table 1), and K_h is the hydrolysis kinetic constant. The molecular weight is related to C_E and C_C [2]

$$C_C = \frac{\rho}{M_n} \tag{6}$$

$$C_E = \frac{\rho}{M_n}(DP-1) \tag{7}$$

In eqs. 6 and 7 ρ is the density of the polymer sample (about 1210 kg/m³) and DP is the average degree of polymerization, defined as the ratio M_n/M (M is the molecular weight of

the repeating unit, equal to 72 g/mol in our case). After replacing eqs. 6 and 7 in eq. 5, considering that *DP* is much larger than 1, one obtains a simple evolution of molecular weight with time

$$M_n = M_{n0} \exp\left(-\frac{\rho C_{A0}}{M} K_h t\right) \qquad (8)$$

If K_h is taken as 2.3 10^{-10} (mol/m^3)$^{-2}$h^{-1} the result reported in Fig. 2 as a continuous line is obtained. The value of the time constant $M/\rho C_{A0} K_h$ is about 300 h, which gives the timescale of the phenomenon. It can be noticed that the equation presents a considerable predicting capability since it correctly describes the experimental points collected at longer times.

According to the results reported in Fig. 2, the hydrolytic scission at 58 °C is nearly negligible during the first about 30 h, and becomes significant (nearly dramatic) after about 100 h.
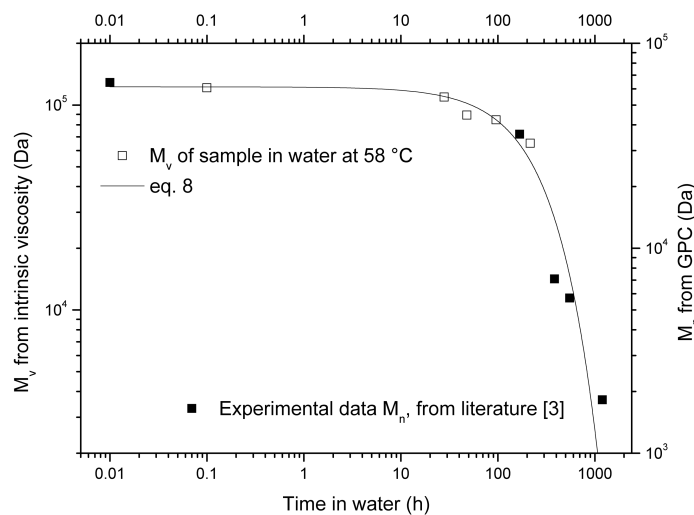
Fig. 2 Time dependence of molecular weight calculated by intrinsic viscosity (left axis). Also, data of number average molecular weight (right axis) taken from the literature [5] are reported as a reference.

Opacity

One evident phenomenon taking place when PLA samples are immersed in water is opacification (and whitening) [11, 13, 23-25]. Fig. 3 reports a picture of a series of films taken out from water at 58 °C at selected time intervals.

$$T = 58\ ^{\circ}C$$

2 h   4 h   8 h   28 h   48 h   73 h   96 h   192 h
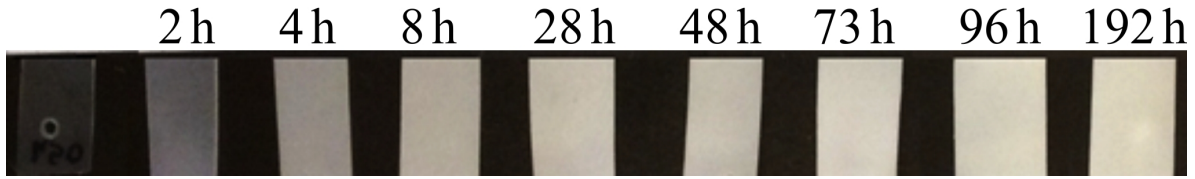
Fig. 3 Images of PLA films taken out from water at 58 °C at selected time intervals. The sample on the left was not immersed in water.

The results of opacity measurements at all the conditions investigated is reported as symbols in Fig. 4. The starting opacity of the samples was about 10% (amorphous PLA film). The opacity of a sample crystallized from the solid amorphous state at the temperature of 100 °C for 5 h is reported as a horizontal line in Fig. 4A. The crystalline amount of such sample was about 45% [14]. It can be noticed that crystallinity increases opacity so that the crystalline sample reaches a value of 20%.

A   B
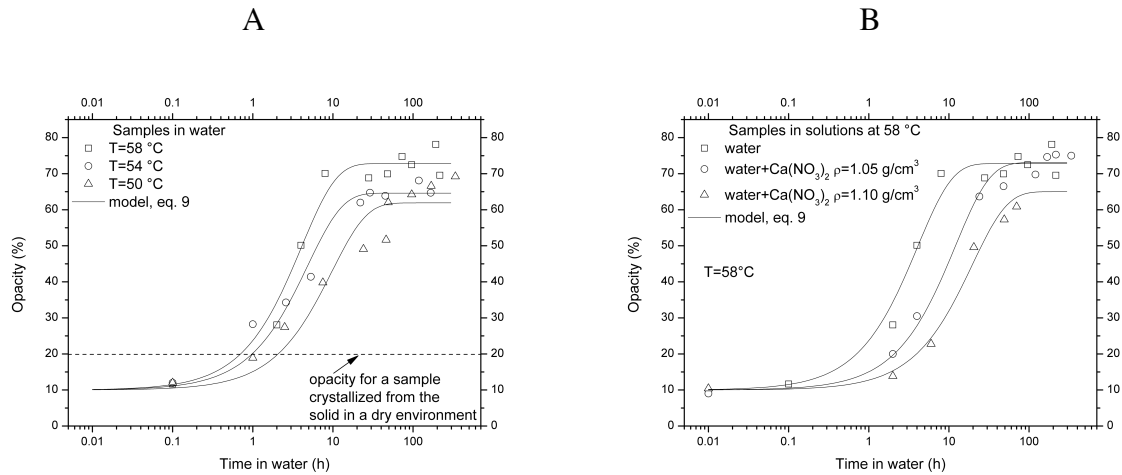
Fig. 4 Opacity of the samples immersed in (A) water at different temperatures and (B) in solutions of water and calcium nitrate at 58 °C as a function of time. The lines refer to the result of eq. 9.

Opacity increases with time of immersion in water, reaching a plateau value in a time which increases with decreasing temperature. The rate of increase of opacity decreases on decreasing temperature (Fig. 4A) and on decreasing the water activity (namely on increasing the salt concentration, shown in Fig. 4B). The plateau value reached (of about 60-70%) is significantly higher than that reached by the crystalline sample: it is clear that the phenomenon cannot be entirely ascribed to crystallization.

The experimental data can be described by a phenomenological equation:

$$\frac{dO_p}{dt} = -\frac{O_p - O_{p\infty}}{\tau} \tag{9}$$

whose results are reported as lines in Fig. 4. In eq. 9, $O_{p\infty}$ is the value reached at long times, and τ is a constant, whose values can be found by a best fitting analysis of experimental data. This equation allows determining the half-time of the phenomenon, $t_{1/2,op}$, as the time at which an opacity equal to one half of the final value $O_{p\infty}$ is reached.
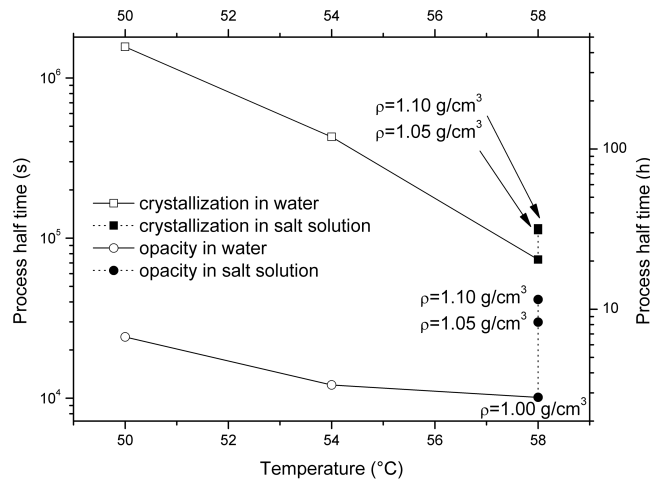
Fig. 5 Process half-times for opacity (both in water and in salt solutions at different concentrations of calcium nitrate tetrahydrate) and for crystallinity.

The results are reported in Fig. 5 versus the temperature of the test. Also, the effect of solution density (namely of a different salt concentration) is reported as solid symbols. The phenomenon of opacification depends on temperature, with $t_{1/2,op}$ increasing from about 2 h at 58 °C to about 6 h at 50 °C. The effect of salt concentration is dramatic: on decreasing the density from pure water (1.49 g of water/100 g of polymer) to 1.1 g/cm^3 (1.29 g of water/100 g of polymer) $t_{1/2,op}$ increases from about 2 h to more than 10 h, namely a factor of about 6 for a decrease of water content of about 15%. If one applies the same rate of change and considers the maximum water content reached in humid air (at a RH of about 90%) according to Fig. 1, namely about 1.05 g of water/100 g of polymer, $t_{1/2,op}$ should be about 170 h, which is consistent with the fact that in humid air opacification was not evident after about 100 h.

It is generally believed [26, 27], that opacification and whitening are results of hydrolytic degradation, which induces a change in the refraction index of the sample as a consequence of water absorption and/or the presence of products formed by the hydrolytic process.

However, it is evident that the phenomenon of opacification reaches a plateau at times at which hydrolysis is still negligible.

Crystallinity

It is quite well known that water can decrease the glass transition temperature of PLA and induce crystallization at temperatures much lower than the nominal glass transition temperature, T_g, of the material reported to be about 60 °C [5]. Fig. 6A reports a comparison between two DMA curves of PLA films analyzed in water and in air under the same conditions (heating at 2 °C/min, tensile mode, 1 Hz). It can be noticed that the sample immersed in water undergoes an anticipated reduction of the storage modulus. The maximum value of the parameter tan(δ), which is often considered an indication of the T_g, is reached at a temperature about 15 °C lower than what measured on the sample kept in the air. It can be noticed that the modulus of the sample immersed in water starts to increase again at a temperature of about 75 °C. This increase can be ascribed to crystallinity, and it is interesting to notice that, when compared to the sample in air, this increase takes place at lower temperatures and is much steeper. On the basis of this behavior, it can be stated that water can considerably lower the T_g of PLA and that crystallinity is surely favored by the plasticizing effect of water. In order to verify the ability of the sample to crystallize in the presence of water, an isothermal DMA test at 58 °C was conducted on a PLA film immersed in water. The results of the analysis are reported in Fig. 6B. The modulus initially decreases during the first about 2 h, probably because of the plasticizing effect of water. An increase is then measured until a plateau is reached after about 30 h. This modulus increase (of factor 10 with respect to the initial value) can be ascribed to crystallinity [28].
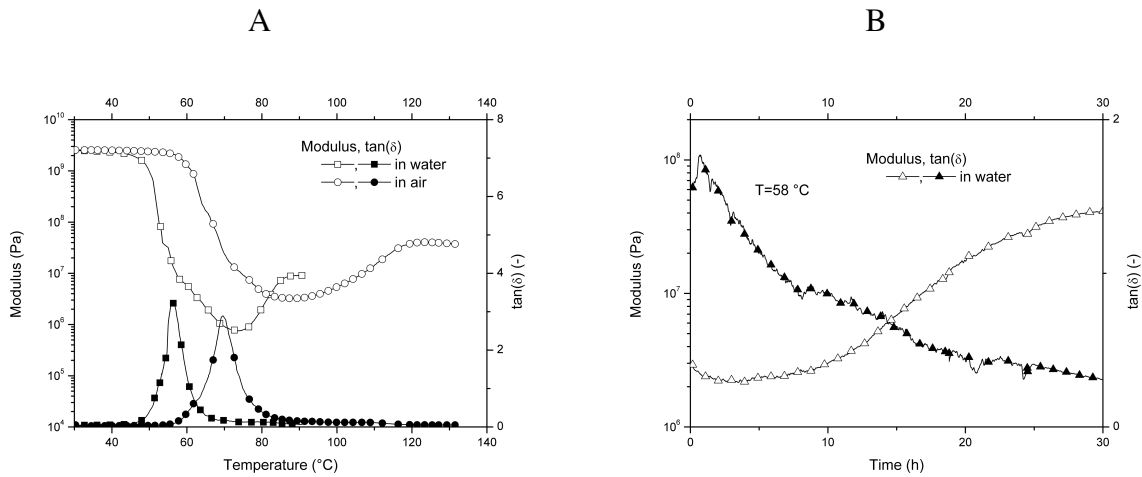
Fig. 6 (A) DMA during heating in the water and in the air; (B) DMA in isothermal conditions in water.

As described in the Experimental section above, the PLA films immersed in water and salt solutions were taken out at selected intervals and analyzed by DSC.

The DSC thermograms of the samples are reported in Fig. 7. All the thermograms refer to the first heating from room temperature to 200 °C, at a heating rate of 10 °C min^{-1}, of samples immersed in different solutions and for different times. In particular, the effect of temperature can be evinced by comparing Fig. 7 from A to C, whereas the effect of water activity at 58 °C can be observed comparing Fig. 7C and D. For all the samples, after a few hours of contact with water, the cold crystallization peak results to be more evident with respect to the starting samples and is located at lower temperatures (about 100 °C, whereas for the starting temperature it was at about 120 °C). The glass transition temperature is clearly detected in all samples at shorter immersion times, and disappears at times which depend on temperature and on water activity. This phenomenon can be ascribed to the increase of crystallinity degree.

The crystallinity degree was calculated from the thermograms measured during the first heating scan according to the equation

$$\chi(t) = \frac{\Delta H(t)}{\Delta H_\infty} = \int_0^t \frac{\delta Q}{\delta t} dt \bigg/ \int_0^{t_\infty} \frac{\delta Q}{\delta t} dt \qquad (10)$$

in which $\delta Q/\delta t$ is the heat flow measured by the calorimeter, $\Delta H(t)$ is the integral of the heat flow after the baseline subtraction, and ΔH_∞ is the latent heat of crystallization of a fully crystalline PLA, which can be found in the literature to be 93 J/g [29, 30].

The values found are reported against the immersion time in Fig. 8. As expected (Fig. 8A) the crystallinity evolution is slower on decreasing the temperature. For the same temperature (Fig. 8B) the decrease of water activity marginally changes (decreases) the evolution rate.

The crystallinity evolution was described by the following Avrami equation [31-34]

$$\chi(t) = \chi_{max} \left[1 - \exp\left[-\ln(2) k^n t^n \right] \right] \tag{11}$$

in which χ_{max}, k and n were kept constant for each condition (either solution or temperature). When written in this form, the kinetic constant k has the meaning of the reciprocal of the half-crystallization time [34], namely

$$t_{1/2,\chi} = 1 / k(T) \tag{12}$$

The lines resulting from the fitting of the data are reported in Fig. 8.
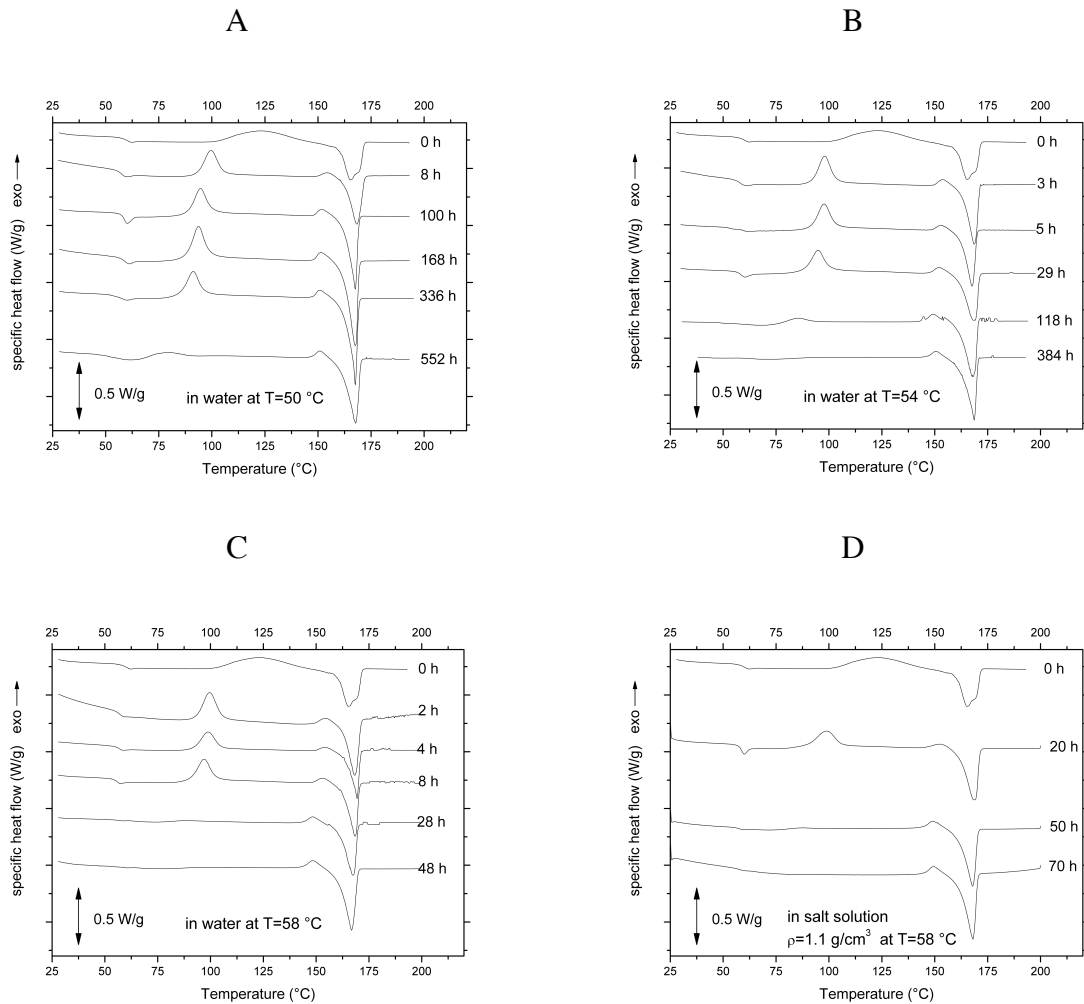
Fig. 7 Calorimetric analysis of samples immersed for different times (A) in water at 50 °C, (B) in water at 54 °C, (C) in water at 58 °C and (D) in the salt solution having a density of 1.1 g/cm³ at 58 °C.

The half-crystallization times are reported in Fig. 5. It can be noticed that the timescales of the two phenomena are completely different: opacity develops over a much shorter timescale.
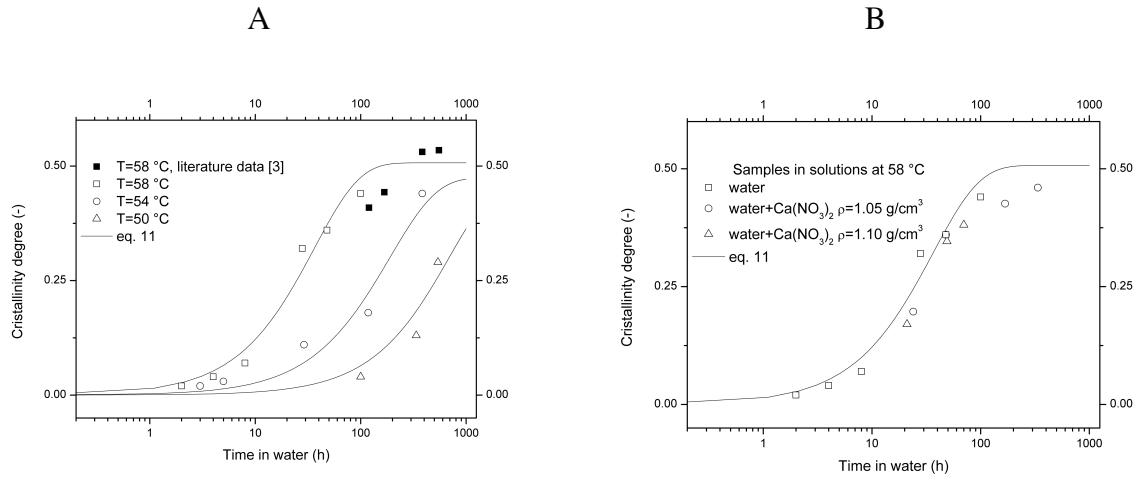
Fig. 8 Evolution with time of crystallinity degree for samples (A) immersed in water at different temperatures and (B) immersed in salt solutions having different densities. The continuous lines refer to the fitting obtained by eq. 11.

The Avrami indexes found from the fitting through eq. 11 are close to 1 for all the tests analyzed in this work. Such a value for the Avrami index is consistent with a nucleation-dominated mechanism in which the crystals are generated on a surface and grow along one direction.

The density measurements carried out on the samples are reported in Fig. 9. The density of the crystalline sample is also reported as a reference. As expected, crystallinity induces an increase of density. However, the samples immersed in water, though presenting a considerable degree of crystallinity, have densities which decrease on increasing the immersion time. This phenomenon is consistent with the presence of crazes inside the sample. These crazes could act as effective nucleation surfaces and thus could justify the Avrami exponent of 1 found from the analysis of crystallinity data.
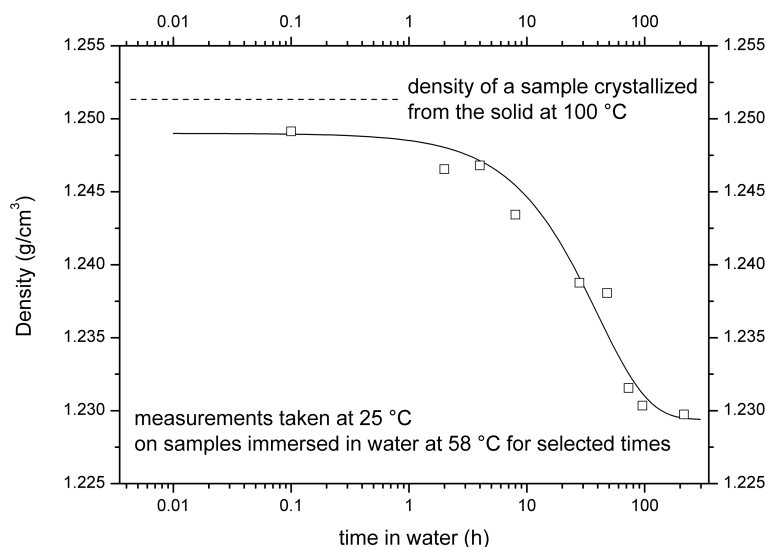
Fig. 9 Measurements of density (at a temperature of 25 °C) of samples immersed for different times in water at 58 °C. The line is just a guide for the eye.

Structural and morphological analysis

The water induced crystallization of initially amorphous PLA samples at 58 °C was directly probed by performing WAXS measurements (Fig. 10A). As shown by the X-ray diffraction profiles of Fig. 10A, the PLA samples immersed in water for less than 6 h are still amorphous (curves a, b) as the initial samples. Crystallization starts occurring after 6 h of water immersion, as indicated in the diffraction profile c of Fig. 10A by the presence of a peak of low intensity at $d \approx 5.4$ Å ($2\theta \approx 16.3°$). The relative intensity of the peak at $d \approx 5.4$ Å increases with increasing the immersion time, and in the case of the samples immersed for 24 and 48 h in water (curves d and e of Fig. 10A, respectively) additional diffraction peaks at $d \approx 4.8$ and 6.1Å ($2\theta \approx 14.6$ and 18.6°, respectively) are also present. The diffraction peaks at $d \approx 4.8, 5.4$ and 6.1 Å correspond to the 010, 200/110 and 203 reflections of the α' disordered modification of PLA, where the indexing of the observed reflections is based on the crystal structure of the ordered α form [35-38]. Therefore, in agreement with DSC results (Fig. 7 and 8), WAXS data (Fig. 10) indicate that after an induction time of $\approx$2-4 h, the immersion of initially amorphous PLA samples in a water bath at 58°C induces crystallization of the α' disordered form.

The SAXS data recorded simultaneously to the WAXS profiles of Fig. 10A, after normalization for the sample thickness, are reported in Fig. 10B.
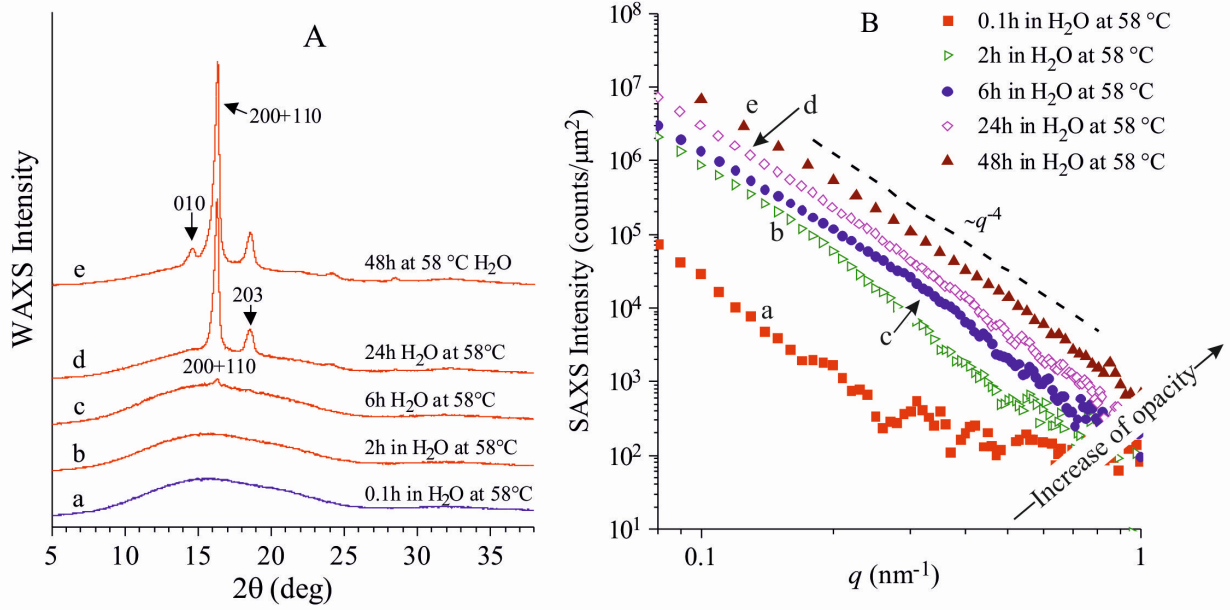
Fig. 10 X-ray scattering profiles at wide (WAXS, A) and small (SAXS, B) angle of PLA samples recorded after immersion in a water bath at 58 °C for different amounts of time. The 010, 200/110 and 203 reflections of α' disordered form of PLA are indicated in A. The power law dependence of SAXS intensity in the tail region according to q^{-4} is indicated in B.

In Fig. 10B, it is apparent the scattering intensity in the small angle region I_{SAXS} of all the water treated samples (Fig. 10B) does not present particular features, but only an asymptotic decay proportional to q^{-4} is observed, which follows the Porod law, that is $I_{SAXS} = K q^{-4}$, with K proportional to the Porod constant K_p. In particular, the SAXS intensity distribution is featureless also in the case of the crystalline samples kept in water for 24 and 48h (curves d,e of Fig. 10B), and only the q^{-4} decaying is observed. Since these samples are crystallized in the disordered α' form, the absence of a correlation peak due to the lamellar periodicity expected for semicrystalline polymers is essentially due to the similar electron density of α' form and amorphous phase [35-38].

The most important characteristic of the SAXS data of Fig. 10B consists in the fact that the SAXS intensity of the samples at any q seems to increases with increasing the permanence time in the water bath at 58 °C. This increase may not be due to PLA crystallization, but it is rather due to the formation of crazes and voids inside the samples. The size of these void should be much higher than $D_{max} \approx 2\pi/q_{min} \approx 80$ nm, where q_{min} is the minimum value of q accessible in our experimental setup (equal to $q_{min} \approx 0.08$ nm^{-1}) and, therefore, D_{max} is the maximum size of any structural feature that can be measured with confidence.

These considerations suggest that our samples may be treated as systems consisting of two phases. One phase is constituted by the amorphous regions of PLA coupled with crystalline regions of α' disordered form, the electron density of which are nearly identical. The second phase instead is constituted by the voids embedded in the PLA matrix, which are created by the effect of water sorption. As a consequence, the q^{-4} decay of the SAXS intensity in the sampled q range may be considered as the tail region of the scattering intensity of a hypothetical two-phase system characterized by sharp interfaces [19]. In order to extract quantitative information, after subtraction of the background (eq. 4), the SAXS data of each sample was normalized for the corresponding total scattered intensity Q measured in the q region between q_{min}=0.08 and q_{max}=1.0 nm^{-1}, calculated as:

$$Q = \frac{1}{2\pi} \int_{q\min}^{q\max} I_{SAXS} q^2 dq \qquad (13)$$

The fit of the so obtained normalized data to the Porod law gives values of an apparent Porod constant K_p equal to 0.19, 0.28, 0.33 and 0.33 nm^2/nm^3 for the samples kept in water for 2 h, 6 h, 24 and 48 h. For a two phase system, the Porod constant is proportional to the surface area at the interface. Therefore, the increase of the apparent Porod constant is parallel with the decrease of density (Fig. 9), confirming that the main effect of water penetration inside PLA in the first 48 h of contact time is not only crystallization but also the formation of voids of size much higher than 80 nm.

The presence of voids was confirmed by FESEM analysis (Fig. 11). As an example the surface FESEM images of PLA films subjected to 48 h immersion in water at 58 °C (Fig. 11D, D') are compared with those of an amorphous samples (Fig. 11A) and of crystalline PLA samples obtained by crystallization from the melt (Fig. 11B) and by annealing the amorphous phase (Fig. 11C) (crystallization conditions 3 h at 105 °C). It is apparent that the surface of the water treated samples is populated by large and small holes, visible also at small magnification (Fig. 11D and D'). In contrast, the surface of the amorphous and the melt crystallized samples appear homogeneous even at large magnification (Fig. 11A,B), whereas the surface of the annealed amorphous sample is characterized by the presence of small holes, having the size of 10-50 nm (Fig. 11B).

FESEM micrographs were collected also at the surface of water treated PLA samples (48 h immersion at 58 °C) subjected to etching with a basic solution (60:40 vol:vol water-methanol mixture, 0.5 M NaOH) for a short time. Two etching conditions were utilized, 30 min at 58 °C and 10 min at 65 °C. Since the base-catalyzed hydrolysis of the ester groups for

the chains located in the amorphous regions is faster than in the crystals, the removal of the amorphous phase upon etching for a short time at temperatures close to the glass transition allows for the visualization of the crystalline morphology developed during the 48 h water immersion. At low magnification (Fig. 11 E,F) globular entities are apparent, that at higher magnification reveal an exfoliated texture (Fig. 11E') and/or stick-like entities radially organized around holes (Fig. 11F'). The radial organization of the sticks around holes suggests that the PLA crystallization during the prolonged water immersion is nucleated around the voids, and it is facilitated by the increase of chain mobility due to the plasticization effect of the water.
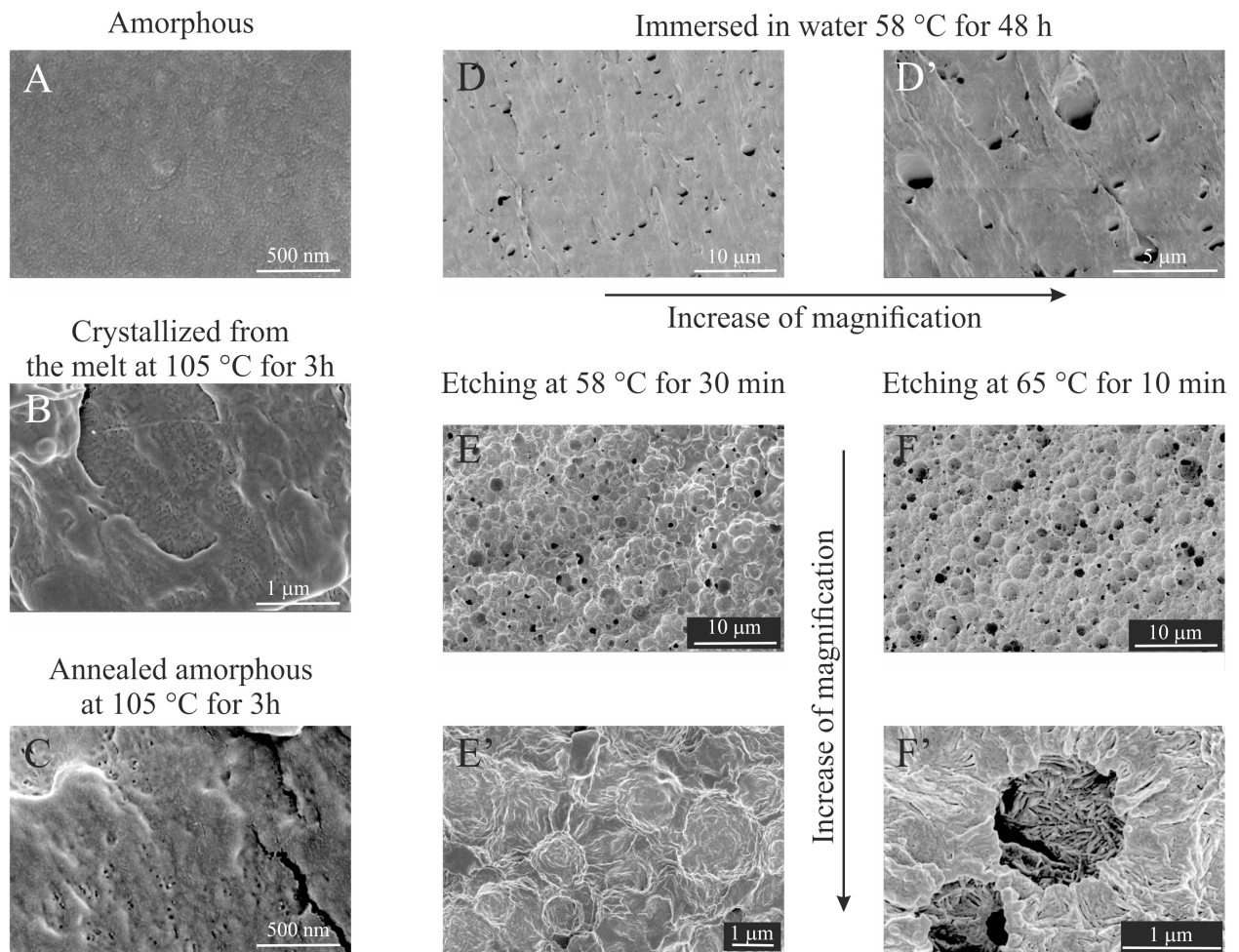
Fig. 11 Comparison between the FESEM images taken at the surface of an amorphous PLA sample (A), a melt crystallized sample (B) and of a sample crystallized by annealing an amorphous film (C) with the surface images of a PLA sample subjected to water immersion for 48h at 58 °C (D-F, D'-F'), before (D,D') and after etching with a basic water solution (60 vol% water, 40 vol % methanol 0.5 M NaOH) for 30 min at 58 °C (E,E') and for 10 min at 65 °C (F,F').

The physical reasons for the formation of these voids, or crazes, induced in PLA by the sorption of water should be further analyzed. Indeed, it is quite well known that a solvent can generate crazes during absorption in glassy polymers [39]. This phenomenon is accepted to be due to the stresses induced by the swelling at the solvent front. This is likely to happen when water penetrates PLA at high temperature, and as shown above it takes places on a timescale consistent with water sorption. It cannot be excluded that the regions around these crazes could present a local rate of hydrolysis different from the bulk of the polymer. Similarly, it is possible that the presence of additives or residues of polymerization can

enhance the phenomenon of craze formation. However, though it is generally reported that the crazes (or cracks) in PLA are produced as a consequence of hydrolysis, from the results obtained in this work it seems that the phenomenon of craze formation takes place at much shorter times than hydrolysis.

Conclusions

Water has a dramatic effect on PLA even at the temperature significantly lower than the nominal glass transition temperature. At surprisingly short times, opacity increase is the first phenomenon to appear, on a timescale consistent with water sorption. This phenomenon seems to be due to crazes induced by water, on their turn originated by the stresses caused by swelling at the penetrating front. The presence of these voids has been assessed in this work by several techniques (density measurements, SAXS, and direct SEM observation). The characteristic times at which opacity and crystallinity develop increase on decreasing temperature and water content. The effect of water content is quite significant: the opacification half time increases by a factor of more than 5 for a reduction of the water content of about 15%. The second phenomenon to become evident is the crystallinity evolution. Crystallinity increases with time showing an Avrami index of about 1, which is consistent with a heterogeneous nucleation on the crazes. These two phenomena take place before hydrolysis becomes significant. Obviously, it is possible that hydrolysis takes part to the two phenomena, but it is questionable if hydrolysis can be their cause.

Acknowledgements

References

1. Lim LT, Auras R, and Rubino M. Progress in Polymer Science 2008;33(8):820-852.
2. Speranza V, De Meo A, and Pantani R. Polymer Degradation And Stability 2014;100(1):37-41.
3. De Santis F and Pantani R. Journal of Polymer Research 2015;22(12):1-9.
4. Pantani R, De Santis F, Sorrentino A, De Maio F, and Titomanlio G. Polymer Degradation And Stability 2010;95(7):1148-1159.
5. Gorrasi G and Pantani R. Polym. Degrad. Stab. 2013;98(5):1006-1014.

6. Hoglund A, Hakkarainen M, and Albertsson A-C. Biomacromolecules 2009;11(1):277-283.

7. Xu H, Yang X, Xie L, and Hakkarainen M. Biomacromolecules 2016;17(3):985-995.

8. Höglund A, Odelius K, and Albertsson A-C. ACS applied materials & interfaces 2012;4(5):2788-2793.

9. Husárová L, Pekařová S, Stloukal P, Kucharzcyk P, Verney V, Commereuc S, Ramone A, and Koutny M. International journal of biological macromolecules 2014;71:155-162.

10. Commereuc S, Askanian H, Verney V, Celli A, and Marchese P. About durability of biodegradable polymers: structure/degradability relationships. Macromolecular symposia, vol. 296: Wiley Online Library, 2010. pp. 378-387.

11. Benali S, Aouadi S, Dechief A-L, Murariu M, and Dubois P. Nanocomposites 2015;1(1):51-61.

12. Fortunati E, Armentano I, Iannoni A, Barbale M, Zaccheo S, Scavone M, Visai L, and Kenny J. Journal Of Applied Polymer Science 2012;124(1):87-98.

13. Pantani R and Sorrentino A. Polymer Degradation And Stability 2013;98(5):1089-1096.

14. Gorrasi G, Anastasio R, Bassi L, and Pantani R. Macromol. Res. 2013;21(10):1110-1117.

15. Davis EM, Theryo G, Hillmyer MA, Cairncross RA, and Elabd YA. ACS applied materials & interfaces 2011;3(10):3997-4006.

16. Solomon OF and Ciutǎ IZ. Journal Of Applied Polymer Science 1962;6(24):683-686.

17. Pamies R, Cifre JGH, Martínez MdCL, and de la Torre JG. Colloid and Polymer Science 2008;286(11):1223-1231.

18. Perego G, Cella G, and Bastioli C. J Appl Polym Sci 1996;59(1):37-43.

19. Roe RJ. Methods of X-ray and Neutron Scattering in Polymer Science: Oxford University Press, 2000.

20. De Santis F, Gorrasi G, and Pantani R. Polymer testing 2015;44:15-22.

21. Gorrasi G, Vittoria V, Murariu M, Ferreira ADS, Alexandre M, and Dubois P. Biomacromolecules 2008;9(3):984-990.

22. Han X, Pan J, Buchanan F, Weir N, and Farrar D. Acta biomaterialia 2010;6(10):3882-3889.

23. Paul MA, Delcourt C, Alexandre M, Degée P, Monteverde F, and Dubois P. Polymer Degradation And Stability 2005;87(3):535-542.

24. Fukushima K, Abbate C, Tabuani D, Gennari M, and Camino G. Polymer Degradation And Stability 2009;94(10):1646-1655.

25. Pantani R and De Santis F. Physical changes of poly (lactic acid) induced by water sorption. POLYMER PROCESSING WITH RESULTING MORPHOLOGY AND PROPERTIES: Feet in the Present and Eyes at the Future: Proceedings of the GT70 International Conference, vol. 1695: AIP Publishing, 2015. pp. 020066.

26. Liu L, Li S, Garreau H, and Vert M. Biomacromolecules 2000;1(3):350-359.

27. Li S and McCarthy S. Biomaterials 1999;20(1):35-44.

28. Martin O and Averous L. Polymer 2001;42(14):6209-6219.

29. Fischer E, Sterzel H, and Wegner G. Colloid & Polymer Science 1973.

30. Schmidt SC and Hillmyer MA. Journal of Polymer Science Part B: Polymer Physics 2001;39(3):300-313.

31. Avrami M. The Journal of Chemical Physics 1939;7(12):1103-1112.

32. Avrami M. The Journal of Chemical Physics 1940;8(2):212-224.

33. Avrami M. The Journal of Chemical Physics 1941;9(2):177-184.

34. De Santis F, Pantani R, and Titomanlio G. Thermochimica acta 2011;522(1):128-134.

35.   Zhang J, Tashiro K, Tsuji H, and Domb AJ. Macromolecules 2008;41(4):1352-1357.
36.   Zhang J, Duan Y, Sato H, Tsuji H, Noda I, Yan S, and Ozaki Y. Macromolecules 2005;38(19):8012-8021.
37.   Cho T-Y and Strobl G. Polymer 2006;47(4):1036-1043.
38.   Pan P, Kai W, Zhu B, Dong T, and Inoue Y. Macromolecules 2007;40(19):6898-6905.
39.   Thomas N and Windle A. Polymer 1981;22(5):627-639.